British Journal of Mathematics & Computer Science
3(3): 240-264, 2013

SCIENCEDOMAIN *international*
www.sciencedomain.org

Pseudorandomness in Central Force Optimization

Richard A. Formato[1*]

[1]*Consulting Engineer & Registered Patent Attorney, Cataldo and Fisher, LLC, P.O. Box 1714, Harwich, MA 02645 USA.*

Research Article

Received: 22 February 2013
Accepted: 8 April 2013
Published: 29 April 2013

Abstract

Central Force Optimization is a deterministic metaheuristic for an evolutionary algorithm that searches a decision space by flying probes whose trajectories are computed using a gravitational metaphor. CFO benefits from the inclusion of a pseudorandom component (a numerical sequence that is precisely known by specification or calculation but otherwise arbitrary). The essential requirement is that the sequence is uncorrelated with the decision space topology, so that its effect is to pseudorandomly distribute probes throughout the landscape. While this process may appear to be similar to the randomness in an inherently stochastic algorithm, it is in fact fundamentally different because CFO remains deterministic at every step. Three pseudorandom methods are discussed (initial probe distribution, repositioning factor, and decision space adaptation). A sample problem is presented in detail and summary data included for a 23-function benchmark suite. CFO's performance is quite good compared to other highly developed, state-of-the-art algorithms.

Keywords: Central force optimization; CFO; optimization; metaheuristic; evolutionary algorithm; pseudorandomness; decision space exploration and exploitation.

1 Introduction

This note examines the role of pseudorandomness in Central Force Optimization. CFO is a deterministic Nature-inspired search and optimization metaheuristic for an evolutionary algorithm (EA) based on gravitational kinematics [1-3]. CFO is similar to gradient-based optimization methods as discussed in detail in [4]. Proofs of convergence for CFO and an extended version have been developed [5,6], and the algorithm has been implemented on a GPU using various topologies [7-9]. The algorithm has been successfully applied to a variety of problems, among them: training neural networks [10]; power grid reliability assessment [11]; drinking water distribution networks [12]; solving nonlinear circuits [13]; array synthesis [14,15]; microstrip patch antenna design [16]; multiband slotted bowtie design [17]; rectangular microstrip patch design [18]; microwave broadband absorber design [19]; antenna optimization generally [20]; notched ultra wideband E-shape antenna design [21]; and increasing impedance bandwidth

*Corresponding author: rf2@ieee.org;

[22,23].

CFO analogizes Newton's mathematically precise laws of motion and gravity, so that its underlying equations are equally precise. The algorithm locates the global maxima of an objective function defined on a decision space Ω with unknown topology (landscape). CFO searches Ω by flying a group of probes whose trajectories are computed from two deterministic equations of motion at a series of discrete time steps (iterations). Details of the CFO metaheuristic are in the Appendix. CFO is fundamentally different from Nature-inspired EAs whose underlying equations are inherently stochastic. Particle Swarm Optimization (PSO) and Ant Colony Optimization (ACO) are examples. Their equations are formulated in terms of true random variables, and removing randomness causes these algorithms to fail completely. By contrast, CFO's equations are inherently deterministic. Every CFO run with the same setup returns precisely the same values step-by-step throughout the entire run. Nevertheless, effective implementations benefit from a pseudorandom component that enters the algorithm indirectly, not through its basic equations. Although pseudorandomness is not required in CFO, numerical experiments show that it is an important feature in effective implementations.

A pseudorandom variable is defined here as one whose value is precisely known but arbitrarily assigned. The value can be specified in advance (for example, an arbitrary sequence of numbers) or it can be calculated in a prescribed manner. The variable's randomness derives from the fact that its value is arbitrary and uncorrelated with Ω's topology, not that it is uncertain in the sense of a true random variable. A true random variable's value is calculated from a probability distribution with successive calculations yielding different values that cannot be known in advance. This type of randomness is fundamentally different from CFO's pseudorandomness. Even when CFO includes pseudorandomness, it remains deterministic, always yielding the same result for runs with the same setup. Once a pseudorandom variable is specified, either explicitly or by calculation, its value is known with absolute precision, so that CFO's trajectory calculations are deterministic even in the presence of pseudorandomness. The original CFO implementation did not include a pseudorandom component [1], thereby limiting its ability to explore Ω; but this limitation can be mitigated to some extent by introducing a measure of pseudorandomness. There are many ways this can be accomplished; three simple methods are described here.

2 CFO Methodology

This paper discusses a CFO implementation with pseudorandomness injected in the following ways: (1) the initial probe distribution (IPD); (2) the repositioning factor; and (3) changing the decision space boundaries. The algorithm is referred to as CFO-PR. Every CFO run starts with a user-specified IPD (total number of probes and their locations in Ω at the beginning of the run, step 0). An arbitrary, variable initial probe distribution is a convenient way to inject pseudorandomness, the effect of which is to provide better sampling of Ω's topology than a static distribution. Each initial probe distribution in a set of distributions provides different information about Ω's landscape. As the results below show, certain ones perform much better than others.

The second method of injecting pseudorandomness is the use of a step-by-step variable repositioning factor $\Delta F_{rep} \le F_{rep} \le 1$ where ΔF_{rep} is the step increment. Repositioning refers to the process of retrieving a probe that has flown outside the decision space (discussed in detail in the Appendix). A variable F_{rep} has the effect of pseudorandomly distributing probes throughout

Ω, which provides better sampling of the decision space landscape as a run progresses. The third way pseudorandomness is injected is by shrinking the decision space around the best probe's location. This process coupled with variable F_{rep} redistributes probes in the smaller Ω in an arbitrary but precise, hence pseudorandom, manner. The effect is to speed CFO's convergence, but at the risk of premature convergence (on an empirical basis, this issue does not appear to be significant using the procedures described below). Pseudocode for CFO-PR appears in Fig. 1. The inner time step loop (j loop) is common to all CFO implementations, but the two outer loops inject initial probe pseudorandomness. The γ loop controls where initial probes are deployed, and the N_p/N_d loop determines their number. These two parameters define the initial probe distribution, and the two loops together create a variable, pseudorandom distribution (see Appendix for notation and equations). The variable F_{rep} procedure appears in step (f) of the pseudocode. And the pseudorandom decision space adaptation is in step (g). Ω's boundaries shrink around the then best probe position vector every 20th step as discussed in detail below. A two-dimensional example is used to illustrate these techniques because it provides a concrete visualization of the different methods. In the actual CFO-PR implementation, of course, these techniques are generalized to the N_d -dimensional case.

2.1 Initial Probes

The manner in which initial probes are deployed using γ is shown schematically in Fig. 2, which provides a 2-dimensional (2D) schematic representation of a variable initial probe distribution comprising an orthogonal array of ${}^{N_p}\!/\!{}_{N_d}$ probes per axis deployed uniformly on probe lines parallel to the coordinate axes that intersect at a point along Ω's principal diagonal. N_d is Ω's dimensionality (here $N_d = 2$), and $x_i^{\min} \le x_i \le x_i^{\max}$, $1 \le i \le N_d$ define Ω's domain (decision space).

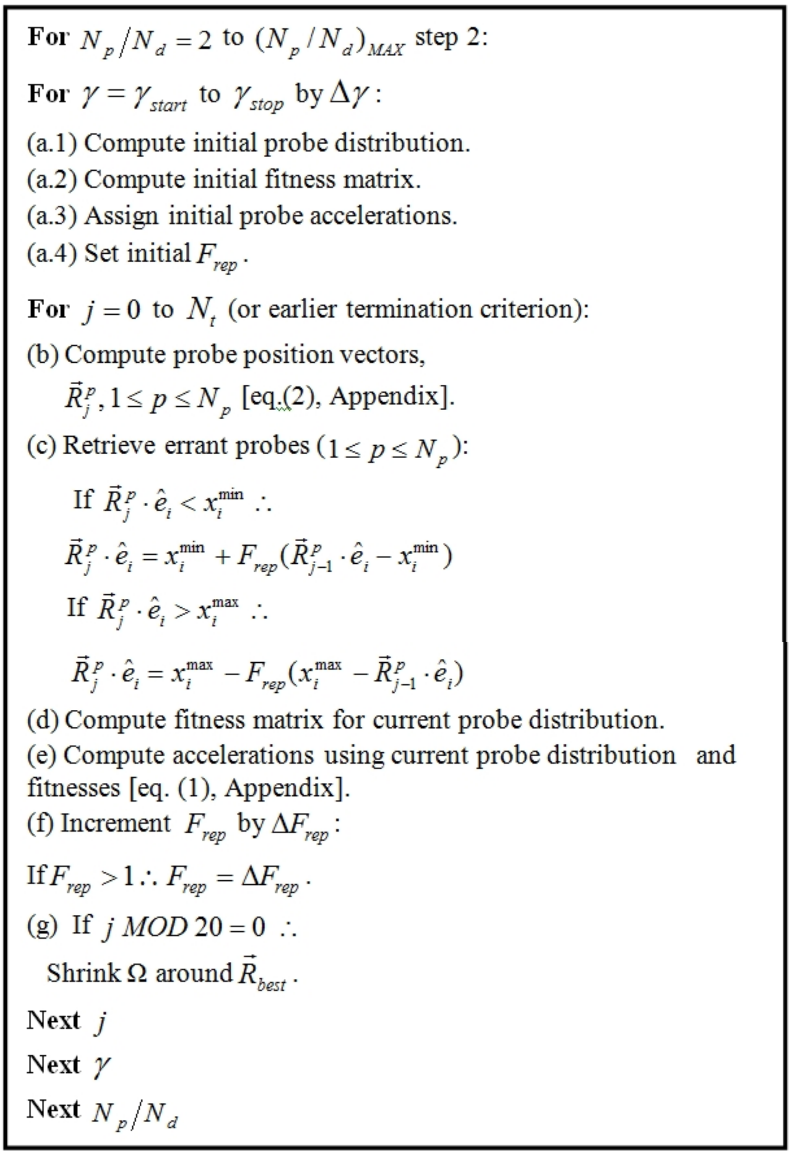

```
For $N_p/N_d = 2$ to $(N_p/N_d)_{MAX}$ step 2:
  For $\gamma = \gamma_{start}$ to $\gamma_{stop}$ by $\Delta\gamma$:
    (a.1) Compute initial probe distribution.
    (a.2) Compute initial fitness matrix.
    (a.3) Assign initial probe accelerations.
    (a.4) Set initial $F_{rep}$.
    For $j = 0$ to $N_t$ (or earlier termination criterion):
      (b) Compute probe position vectors,
          $\vec{R}_j^p, 1 \le p \le N_p$ [eq.(2), Appendix].
      (c) Retrieve errant probes ($1 \le p \le N_p$):
          If $\vec{R}_j^p \cdot \hat{e}_i < x_i^{\min} \therefore$
          $\vec{R}_j^p \cdot \hat{e}_i = x_i^{\min} + F_{rep}(\vec{R}_{j-1}^p \cdot \hat{e}_i - x_i^{\min})$
          If $\vec{R}_j^p \cdot \hat{e}_i > x_i^{\max} \therefore$
          $\vec{R}_j^p \cdot \hat{e}_i = x_i^{\max} - F_{rep}(x_i^{\max} - \vec{R}_{j-1}^p \cdot \hat{e}_i)$
      (d) Compute fitness matrix for current probe distribution.
      (e) Compute accelerations using current probe distribution and
          fitnesses [eq. (1), Appendix].
      (f) Increment $F_{rep}$ by $\Delta F_{rep}$:
          If $F_{rep} > 1 \therefore F_{rep} = \Delta F_{rep}$.
      (g) If $j \; MOD \; 20 = 0 \;\therefore$
          Shrink $\Omega$ around $\vec{R}_{best}$.
    Next $j$
  Next $\gamma$
Next $N_p/N_d$
```

Fig. 1. CFO-PR pseudocode with variable initial probes and F_{rep} and DS adaptation

For illustrative purposes, Fig. 2 shows nine probes on each probe line. The lines, which are parallel to the x_1 and x_2 axes, intersect at a point on Ω's principal diagonal marked by position vector $\vec{D} = \vec{X}_{\min} + \gamma(\vec{X}_{\max} - \vec{X}_{\min})$, where $\vec{X}_{\min} = \sum_{i=1}^{N_d} x_i^{\min}\hat{e}_i$ and $\vec{X}_{\max} = \sum_{i=1}^{N_d} x_i^{\max}\hat{e}_i$ are the diagonal's endpoint vectors. Parameter $0 \le \gamma \le 1$ specifies where along the diagonal the orthogonal probe array is placed by locating the probe lines' intersection point.

While Fig. 2 shows an equal number of probes on each line, a different number of probes per axis can be used instead. For example, if equal probe spacing were desired in a decision space with unequal boundaries, or if overlapping probes were to be excluded in a symmetrical space, then unequal numbers would be used. Unequal numbers also might be appropriate if *a priori* knowledge of Ω's landscape, however obtained, suggests denser sampling in one area. The initial probe distribution in Fig. 2 with variable ${N_p}/{N_d}$ was used for the CFO-PR runs reported here, but any number of other variable initial probe distributions could be used instead. The key idea is that the initial probe distribution must be pseudorandom, that is, arbitrary and therefore uncorrelated with the decision space landscape.

2.2 Repositioning Factor

A variable value for F_{rep} also adds pseudorandomness. F_{rep} starts at some arbitrary initial value that is incremented at each iteration by an arbitrary amount ΔF_{rep} so that $\Delta F_{rep} \le F_{rep} \le 1$. This errant probe retrieval scheme is an example of an arbitrary sequence of calculated numbers deterministically assigned to a CFO parameter. CFO's ability to search the decision space depends on where errant probes are reinserted in Ω, and this process is pseudorandom in nature because F_{rep} is deterministic but arbitrary and uncorrelated with Ω's topology. By placing errant probes pseudorandomly throughout the decision space, more information is developed about its topology as the run progresses. The scheme used here was empirically determined, and appears to work well across a wide range of objective functions. But, of course, there are many other procedures for setting F_{rep}'s value, some no doubt better than others.

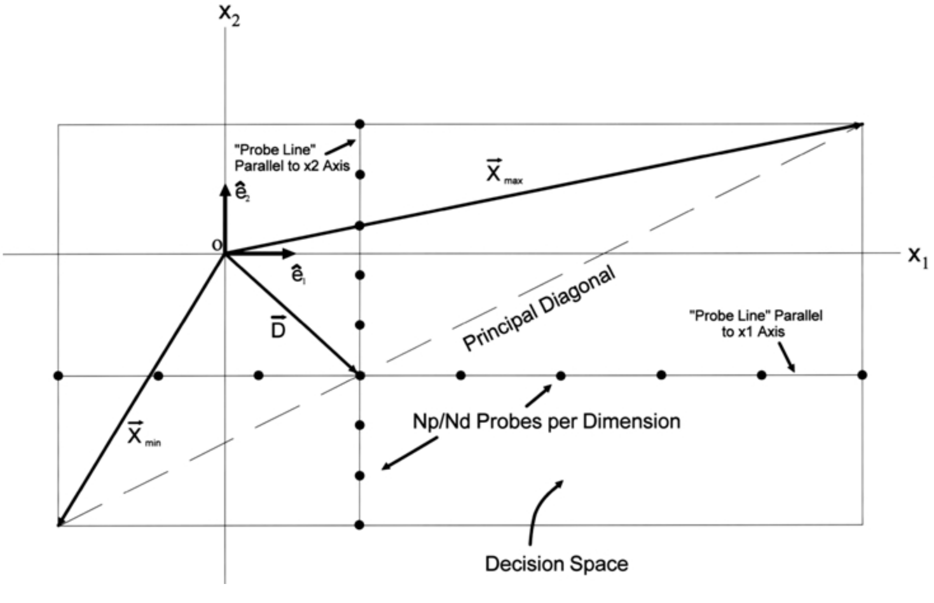
x2
x1
"Probe Line" Parallel to x2 Axis
ê2
ê1
o
X max
D
X min
Principal Diagonal
"Probe Line" Parallel to x1 Axis
Np/Nd Probes per Dimension
Decision Space

Fig. 2. Variable 2-D initial probe distribution used for CFO runs reported here

2.3 Decision Space Adaptation

CFO-PR also includes adaptive reconfiguration of the decision space in order to improve convergence speed. This feature also is pseudorandom in nature because the way Ω's boundaries are changed is arbitrary and uncorrelated with the landscape. Fig. 3 illustrates in 2D how Ω's size is adaptively reduced in this case every 20th step around the probe's location with the then best fitness throughout the run up to the current iteration, $\vec{R}_{best}$. Ω's boundary coordinates are reduced by one-half the distance from the best probe's position to the each boundary on a coordinate-by-coordinate basis, that is, $x_i'^{\min} = x_i^{\min} + \frac{\vec{R}_{best} \cdot \hat{e}_i - x_i^{\min}}{2}$ and $x_i'^{\max} = x_i^{\max} - \frac{x_i^{\max} - \vec{R}_{best} \cdot \hat{e}_i}{2}$, where the primed coordinate is the new decision space boundary, and the dot denotes vector inner product. For clarity, Fig. 3 shows $\vec{R}_{best}$ as fixed, whereas generally it varies throughout a run. Changing Ω's boundary every twenty steps instead of some other interval was chosen arbitrarily (another, probably better approach, might be a reactive adaptation based on performance measures such as convergence speed or fitness saturation).

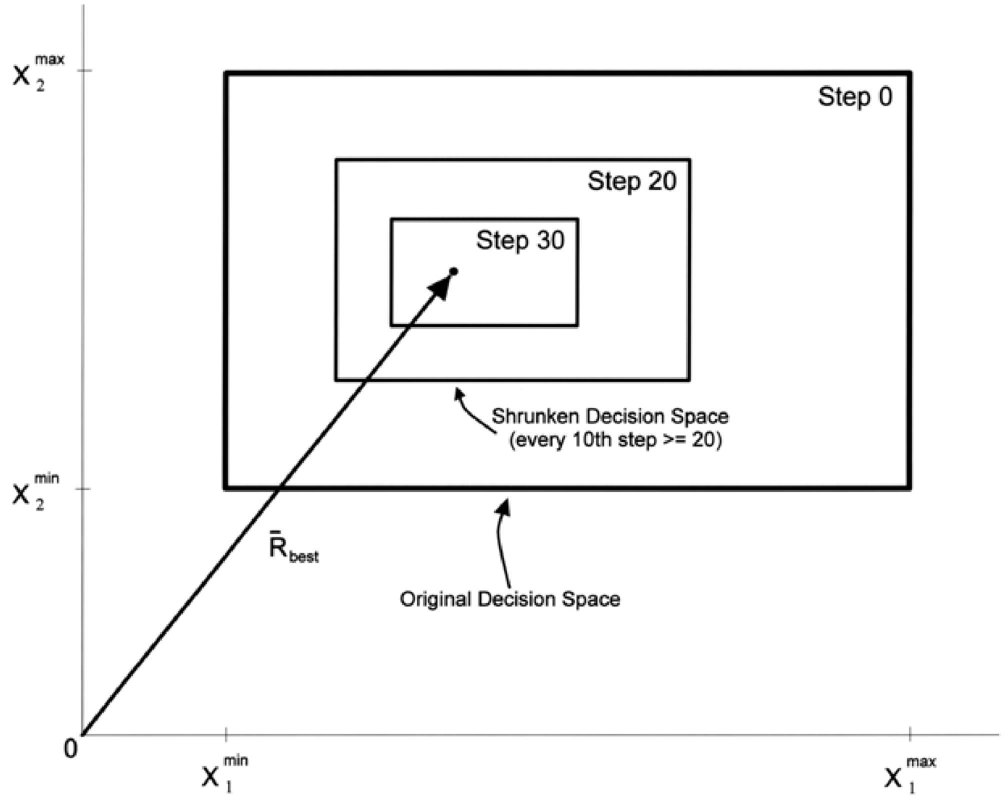

Fig. 3. Schematic 2-D decision space adaptation (with constant $\vec{R}_{best}$)

3 Results and Discussion

3.1 A Sample Problem

The effectiveness of injecting pseudorandomness into CFO-PR will be illustrated with the 2D Goldstein-Price function (GP) plotted in Fig. 4. GP is defined as

$$f(x_1,x_2) = -[1+(x_1+x_2+1)^2\cdot(19-14x_1+3x_1^2-14x_2+6x_1x_2+3x_2^2)] \\ \times[30+(2x_1-3x_2)^2\cdot(18-32x_1+12x_1^2+48x_2-36x_1x_2+27x_2^2)] \quad ,$$

where Ω: $-100 \le x_1, x_2 \le 100$ (note that in most published reports Ω is much smaller, *viz.*, $-2 \le x_1, x_2 \le 2$). GP's global maximum is –3 at (0,–1). This function is multimodal with few local maxima, and it varies over nearly nineteen orders of magnitude as shown in Fig. 4.

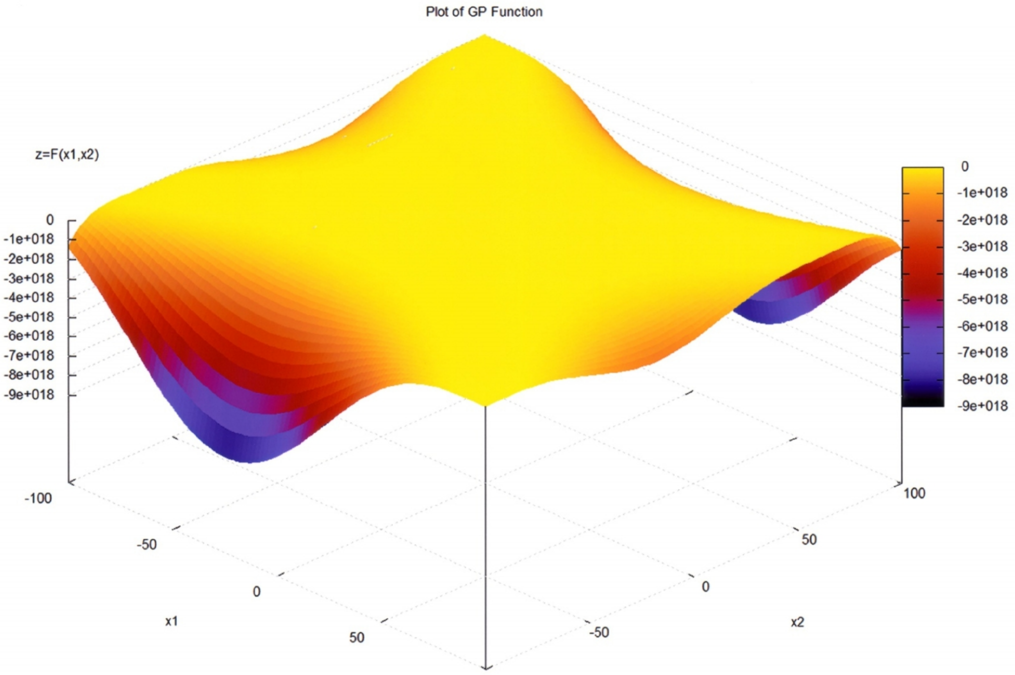

Fig. 4. Goldstein-price (GP) function

The following parameter values were used for all runs reported in this note: $\alpha = 2$, $\beta = 2$, $G = 2$, $\Delta t = 1$, initial acceleration of zero, initial $F_{rep} = 0.5$, $\Delta F_{rep} = 0.05$, $\gamma_{start} = 0$, $\gamma_{stop} = 1$ with $\Delta\gamma = 0.1$ (eleven runs). For GP, $N_p/N_d = 4$ to 14 by 2, with different ranges of this parameter for the other test functions as described below. In all cases, a run was terminated early if the average best fitness over 50 steps (including the current step) and the current best fitness differed by less than 10^{-6}. The pseudorandom IPD's computed using the procedure illustrated in Fig. 2 for GP are plotted in Fig. 5. A further illustration of the Probe Line IPD concept is shown in 3D in Fig. 6.

Table 1 shows a summary of the results for the GP function. A total of sixty-six optimization runs were made in six groups of eleven runs each (data for Run #0 are starting values). The column headings are for the most part self-explanatory. Each run began with $N_t = 500$, but, as the *#Steps* column shows, in no case were 500 iterations used because every run terminated early. N_{eval} is the number of function evaluations performed for the shortened run, and the total number of evaluations over all runs appears at the bottom of this column. The F_{rep} column lists F_{rep}'s value at the end of the run, and the V denotes that F_{rep} was variable as discussed above. *Fitness* tabulates the best fitness returned during the run. The *Initial Probes* column shows the type of IPD, in this case probes uniformly spaced along probe lines parallel to Ω's axes (notated ‖-AXIS) as described above and shown in Fig. 5.

The best fitness ranged from a low of $-236.6643...$ in run 12 to the global maximum of -3 at $(0,-1)$, which was returned in run #54 (best results highlighted in blue). Parameters for run #54 were $N_p / N_d = 12$, $N_p = 24$, and $\gamma = 0.9$. The total number of function evaluations over all runs was $180{,}472$ while N_{eval} for the best run was $1{,}464$ (60 iterations). Fig. 7 plots the evolution of GP's best fitness, which in only two steps increases from $-2.992268247672\text{x}10^{-12}$ to GP's actual global maximum of -3. This seems to be quite remarkable in view of the initial probe distribution for $\gamma = 0.9$ (Fig. 5) in which all probes are far removed from the maximum's location at $(0,-1)$. As the data in Table 1 clearly show, some sets of parameters are much better than others. Without pseudorandom initial probes, a single run would be made with, in this example, only 13.6% probability of locating the global maximum with a fractional accuracy of 0.03% (9 of 66 runs). This statistic highlights the importance of pseudorandomness in CFO.

Fig. 8 plots CFO's D_{avg} curve for GP. D_{avg} is the normalized average distance between the probe with the best fitness and all other probes at each time step, *viz.*, $D_{avg} = \frac{1}{L \cdot (N_p - 1)} \sum_{p=1}^{N_p} \sqrt{\sum_{i=1}^{N_d} (x_i^{p,j} - x_i^{p*,j})^2}$ where $p*$ is the number of the probe with the best fitness, and $L = \sqrt{\sum_{i=1}^{N_d} (x_i^{\max} - x_i^{\min})^2}$ is the length of Ω's principal diagonal (see Appendix for definitions). D_{avg} decreases monotonically through step 10 to 0.0496977, then increases very quickly to a peak of 0.4767301 at step 11, followed by another quasi-monotonic decrease through step 29 to 0.0274355. This cycle repeats through step 48 where D_{avg} is 0.0169657, followed by a jump to 0.1194779 at step 49. After a slight dip through step 53, D_{avg} flattens out around a value of 0.11… The quasi-oscillatory behavior in D_{avg} usually correlates with local trapping, which in this case happens to be at the global maximum. Oscillation in D_{avg} may be a similar phenomenon to oscillation seen in ΔV curves for gravitationally trapped Near Earth Objects (NEOs), where ΔV is the velocity change needed to avoid earth impact, which suggests that NEO theory may hold the key to analytical mitigation or elimination of local trapping at local maxima and possibly another proof of convergence for CFO.

Because CFO-PR converges so quickly on GP's global maximum, the number of the probe with the best fitness is constant after step #1 as seen in the best probe plot in Fig. 9. The best probe number (#14) is the same for steps 0 and 1, but it switches to probe #2 at step 2. Neither the number of the best probe nor the fitness change after step 2. Of course, for most functions the best probe number varies throughout a run, often quite erratically.

Figs. 10 and 11, respectively, plot the probe trajectories for the probes with the best ten fitnesses ordered by fitness and for the first sixteen individual probes ordered by probe number (number of trajectories plotted chosen as a matter of convenience). Both plots are very chaotic with no obvious sign of regularity in how probes gravitate to the global maximum. Nevertheless, there is some measure of regularity as reflected in the D_{avg} curve because its appearance is not nearly as chaotic as the trajectory plots. In fact, in many cases D_{avg} exhibits a mathematically precise oscillation even when the probe trajectories look like Figs. 10 and 11 (see in particular [1]).

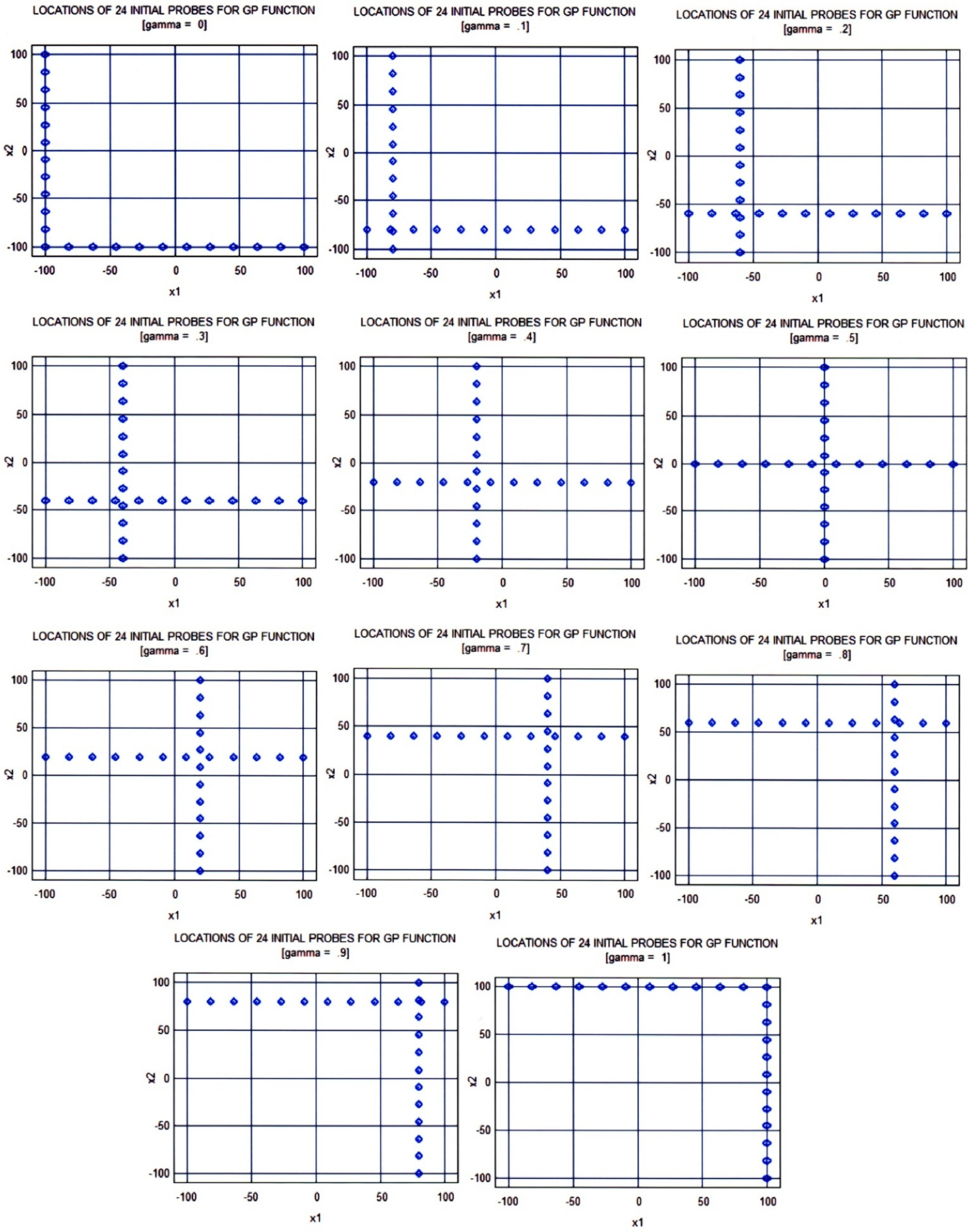

Fig. 5. GP best run initial probe distributions

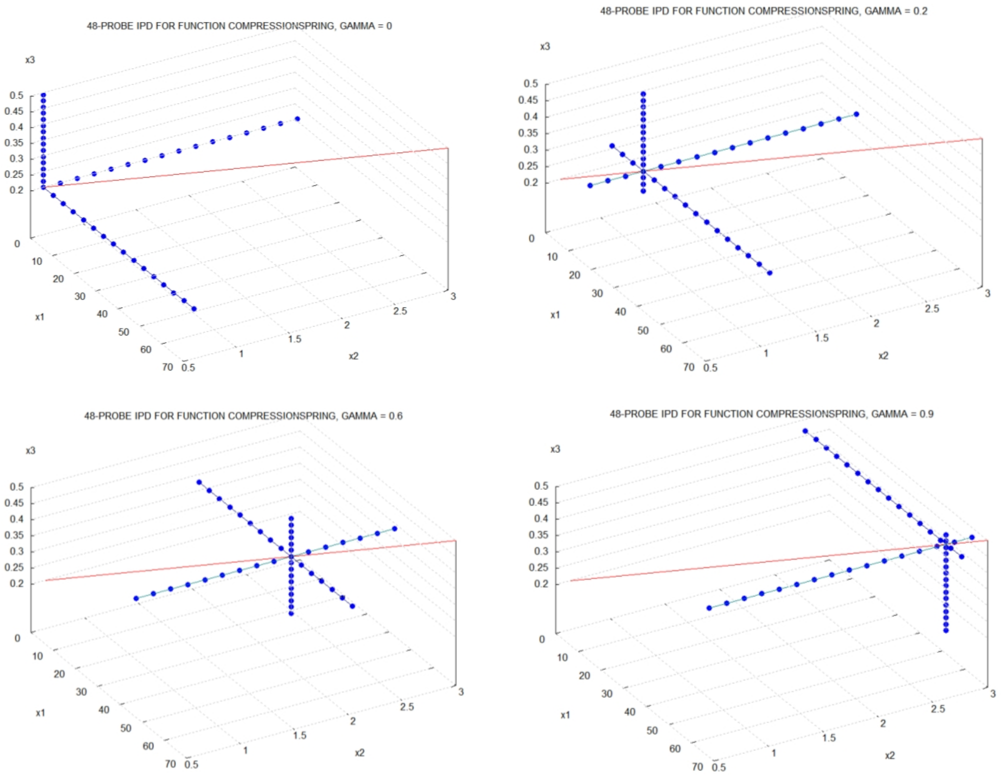

Fig. 6. Example of a 3D probe line IPD

3.2 A Benchmark Suite

CFO was tested against the same twenty-three function 2-30D benchmark suite used to evaluate Group Search Optimizer (GSO) [24]. GSO has gained some notoriety as an effective state-of-the-art stochastic algorithm [25]. In [24] GSO is compared to two other algorithms, PSO and GA, using the benchmark suite described in detail in [26] (functions, decision spaces, and characteristics). PSO is a stochastic Particle Swarm Optimization algorithm implemented using PSOt, a MATLAB-based toolbox that includes standard and variant PSO algorithms. The standard PSO algorithm was used with recommended default parameters: population, 50; acceleration factors, 2.0; inertia weight decaying from 0.9 to 0.4. GA is a stochastic Genetic Algorithm implemented using the GAOT toolbox (Genetic Algorithm Optimization Toolbox). GA also employed recommended default parameter values with a fixed population size (50), uniform mutation, heuristic crossover, and normalized geometric ranking for selection. Thus, while the results reported here compare CFO and GSO directly, they also compare CFO to PSO and GA indirectly.

Table 1 summarizes results using the same function numbering as [24]. $f_{\max}$ is the known global *maximum* (note that the negative of each benchmark in [24] is used here because, unlike the other algorithms, CFO locates maxima, not minima). $<\cdot>$ denotes average value. Because GSO, PSO and GA are inherently stochastic, their performance must be described statistically. Statistical data in Table 2 for those algorithms are reproduced from [24], while Table 3 shows the number of function evaluations per GSO/GA/PSO run. The tabulated fitnesses are average values over 1,000 runs for the first thirteen benchmarks, and over 50 for the others. In marked contrast, CFO's results are repeatable over runs with the same parameters because the algorithm is completely deterministic, even when pseudorandomness is included. CFO therefore never requires a statistical description of its performance, which is a major advantage and a significant departure from the far more common stochastic approaches.

Table 1. Summary results for GP function using pseudorandom CFO-PR

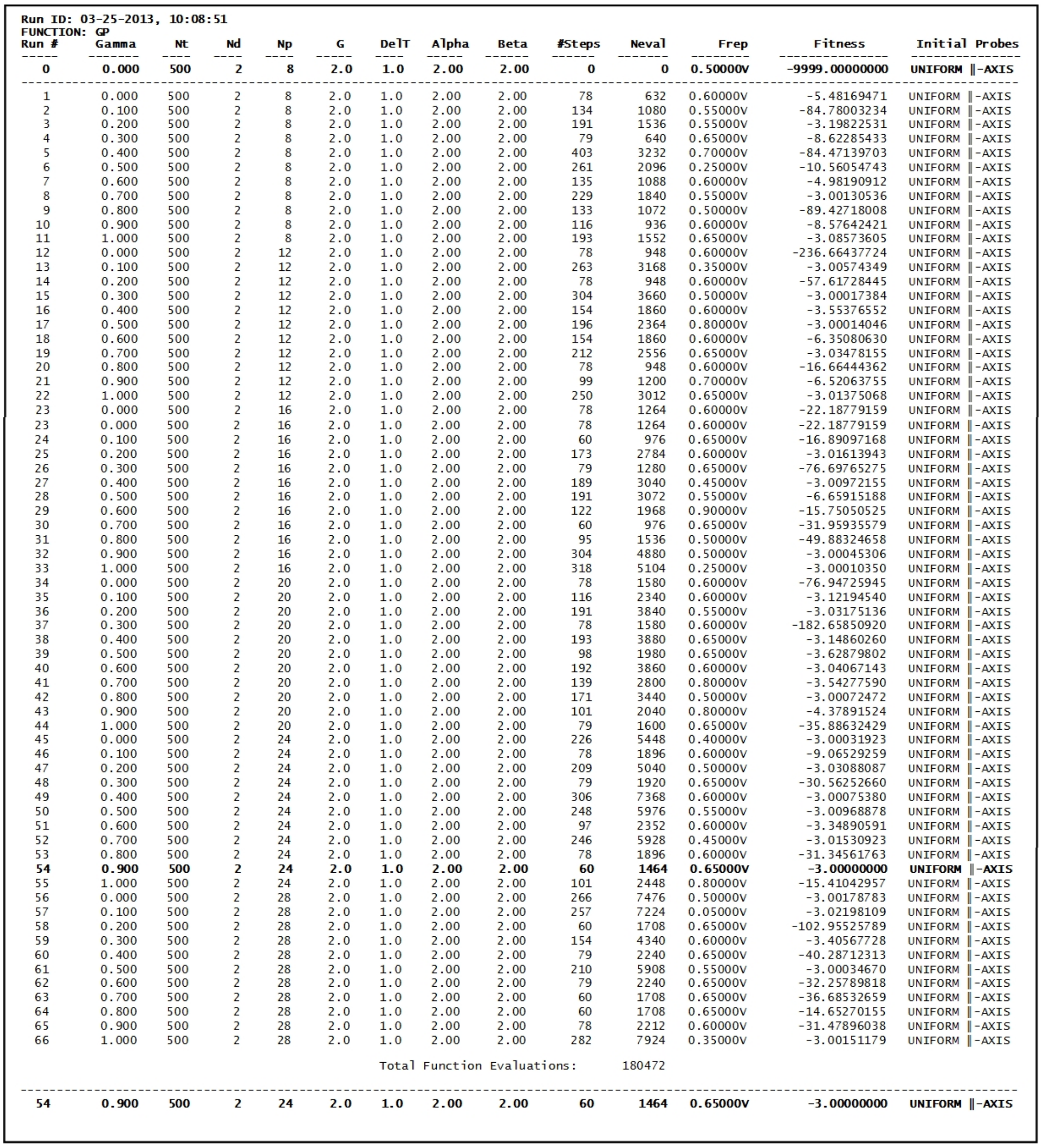

```
Run ID: 03-25-2013, 10:08:51
FUNCTION: GP
Run #    Gamma     Nt     Nd     Np      G     DelT  Alpha    Beta   #Steps   Neval       Frep          Fitness        Initial Probes
-----   -------   ----   ----   ----   -----   ----  -----   ------   ------  -------   --------   ---------------   --------------
  0      0.000    500      2      8     2.0    1.0   2.00    2.00        0        0   0.50000V    -9999.00000000    UNIFORM ‖-AXIS
-----------------------------------------------------------------------------------------------------------------------------------
  1      0.000    500      2      8     2.0    1.0   2.00    2.00       78      632   0.60000V       -5.48169471    UNIFORM ‖-AXIS
  2      0.100    500      2      8     2.0    1.0   2.00    2.00      134     1080   0.55000V      -84.78003234    UNIFORM ‖-AXIS
  3      0.200    500      2      8     2.0    1.0   2.00    2.00      191     1536   0.55000V       -3.19822531    UNIFORM ‖-AXIS
  4      0.300    500      2      8     2.0    1.0   2.00    2.00       79      640   0.65000V       -8.62285433    UNIFORM ‖-AXIS
  5      0.400    500      2      8     2.0    1.0   2.00    2.00      403     3232   0.70000V      -84.47139703    UNIFORM ‖-AXIS
  6      0.500    500      2      8     2.0    1.0   2.00    2.00      261     2096   0.25000V      -10.56054743    UNIFORM ‖-AXIS
  7      0.600    500      2      8     2.0    1.0   2.00    2.00      135     1088   0.60000V       -4.98190912    UNIFORM ‖-AXIS
  8      0.700    500      2      8     2.0    1.0   2.00    2.00      229     1840   0.55000V       -3.00130536    UNIFORM ‖-AXIS
  9      0.800    500      2      8     2.0    1.0   2.00    2.00      133     1072   0.50000V      -89.42718008    UNIFORM ‖-AXIS
 10      0.900    500      2      8     2.0    1.0   2.00    2.00      116      936   0.60000V       -8.57642421    UNIFORM ‖-AXIS
 11      1.000    500      2      8     2.0    1.0   2.00    2.00      193     1552   0.65000V       -3.08573605    UNIFORM ‖-AXIS
 12      0.000    500      2     12     2.0    1.0   2.00    2.00       78      948   0.60000V     -236.66437724    UNIFORM ‖-AXIS
 13      0.100    500      2     12     2.0    1.0   2.00    2.00      263     3168   0.35000V       -3.00574349    UNIFORM ‖-AXIS
 14      0.200    500      2     12     2.0    1.0   2.00    2.00       78      948   0.60000V      -57.61728445    UNIFORM ‖-AXIS
 15      0.300    500      2     12     2.0    1.0   2.00    2.00      304     3660   0.50000V       -3.00017384    UNIFORM ‖-AXIS
 16      0.400    500      2     12     2.0    1.0   2.00    2.00      154     1860   0.60000V       -3.55376552    UNIFORM ‖-AXIS
 17      0.500    500      2     12     2.0    1.0   2.00    2.00      196     2364   0.80000V       -3.00014046    UNIFORM ‖-AXIS
 18      0.600    500      2     12     2.0    1.0   2.00    2.00      154     1860   0.60000V       -6.35080630    UNIFORM ‖-AXIS
 19      0.700    500      2     12     2.0    1.0   2.00    2.00      212     2556   0.65000V       -3.03478155    UNIFORM ‖-AXIS
 20      0.800    500      2     12     2.0    1.0   2.00    2.00       78      948   0.60000V      -16.66444362    UNIFORM ‖-AXIS
 21      0.900    500      2     12     2.0    1.0   2.00    2.00       99     1200   0.70000V       -6.52063755    UNIFORM ‖-AXIS
 22      1.000    500      2     12     2.0    1.0   2.00    2.00      250     3012   0.65000V       -3.01375068    UNIFORM ‖-AXIS
 23      0.000    500      2     16     2.0    1.0   2.00    2.00       78     1264   0.60000V      -22.18779159    UNIFORM ‖-AXIS
 23      0.000    500      2     16     2.0    1.0   2.00    2.00       78     1264   0.60000V      -22.18779159    UNIFORM ‖-AXIS
 24      0.100    500      2     16     2.0    1.0   2.00    2.00       60      976   0.65000V      -16.89097168    UNIFORM ‖-AXIS
 25      0.200    500      2     16     2.0    1.0   2.00    2.00      173     2784   0.60000V       -3.01613943    UNIFORM ‖-AXIS
 26      0.300    500      2     16     2.0    1.0   2.00    2.00       79     1280   0.65000V      -76.69765275    UNIFORM ‖-AXIS
 27      0.400    500      2     16     2.0    1.0   2.00    2.00      189     3040   0.45000V       -3.00972155    UNIFORM ‖-AXIS
 28      0.500    500      2     16     2.0    1.0   2.00    2.00      191     3072   0.55000V       -6.65915188    UNIFORM ‖-AXIS
 29      0.600    500      2     16     2.0    1.0   2.00    2.00      122     1968   0.90000V      -15.75050525    UNIFORM ‖-AXIS
 30      0.700    500      2     16     2.0    1.0   2.00    2.00       60      976   0.65000V      -31.95935579    UNIFORM ‖-AXIS
 31      0.800    500      2     16     2.0    1.0   2.00    2.00       95     1536   0.50000V      -49.88324658    UNIFORM ‖-AXIS
 32      0.900    500      2     16     2.0    1.0   2.00    2.00      304     4880   0.50000V       -3.00045306    UNIFORM ‖-AXIS
 33      1.000    500      2     16     2.0    1.0   2.00    2.00      318     5104   0.25000V       -3.00010350    UNIFORM ‖-AXIS
 34      0.000    500      2     20     2.0    1.0   2.00    2.00       78     1580   0.60000V      -76.94725945    UNIFORM ‖-AXIS
 35      0.100    500      2     20     2.0    1.0   2.00    2.00      116     2340   0.60000V       -3.12194540    UNIFORM ‖-AXIS
 36      0.200    500      2     20     2.0    1.0   2.00    2.00      191     3840   0.55000V       -3.03175136    UNIFORM ‖-AXIS
 37      0.300    500      2     20     2.0    1.0   2.00    2.00       78     1580   0.60000V     -182.65850920    UNIFORM ‖-AXIS
 38      0.400    500      2     20     2.0    1.0   2.00    2.00      193     3880   0.65000V       -3.14860260    UNIFORM ‖-AXIS
 39      0.500    500      2     20     2.0    1.0   2.00    2.00       98     1980   0.65000V       -3.62879802    UNIFORM ‖-AXIS
 40      0.600    500      2     20     2.0    1.0   2.00    2.00      192     3860   0.60000V       -3.04067143    UNIFORM ‖-AXIS
 41      0.700    500      2     20     2.0    1.0   2.00    2.00      139     2800   0.80000V       -3.54277590    UNIFORM ‖-AXIS
 42      0.800    500      2     20     2.0    1.0   2.00    2.00      171     3440   0.50000V       -3.00072472    UNIFORM ‖-AXIS
 43      0.900    500      2     20     2.0    1.0   2.00    2.00      101     2040   0.80000V       -4.37891524    UNIFORM ‖-AXIS
 44      1.000    500      2     20     2.0    1.0   2.00    2.00       79     1600   0.65000V      -35.88632429    UNIFORM ‖-AXIS
 45      0.000    500      2     24     2.0    1.0   2.00    2.00      226     5448   0.40000V       -3.00031923    UNIFORM ‖-AXIS
 46      0.100    500      2     24     2.0    1.0   2.00    2.00       78     1896   0.60000V       -9.06529259    UNIFORM ‖-AXIS
 47      0.200    500      2     24     2.0    1.0   2.00    2.00      209     5040   0.50000V       -3.03088087    UNIFORM ‖-AXIS
 48      0.300    500      2     24     2.0    1.0   2.00    2.00       79     1920   0.65000V      -30.56252660    UNIFORM ‖-AXIS
 49      0.400    500      2     24     2.0    1.0   2.00    2.00      306     7368   0.60000V       -3.00075380    UNIFORM ‖-AXIS
 50      0.500    500      2     24     2.0    1.0   2.00    2.00      248     5976   0.55000V       -3.00968878    UNIFORM ‖-AXIS
 51      0.600    500      2     24     2.0    1.0   2.00    2.00       97     2352   0.60000V       -3.34890591    UNIFORM ‖-AXIS
 52      0.700    500      2     24     2.0    1.0   2.00    2.00      246     5928   0.45000V       -3.01530923    UNIFORM ‖-AXIS
 53      0.800    500      2     24     2.0    1.0   2.00    2.00       78     1896   0.60000V      -31.34561763    UNIFORM ‖-AXIS
 54      0.900    500      2     24     2.0    1.0   2.00    2.00       60     1464   0.65000V       -3.00000000    UNIFORM ‖-AXIS
 55      1.000    500      2     24     2.0    1.0   2.00    2.00      101     2448   0.80000V      -15.41042957    UNIFORM ‖-AXIS
 56      0.000    500      2     28     2.0    1.0   2.00    2.00      266     7476   0.50000V       -3.00178783    UNIFORM ‖-AXIS
 57      0.100    500      2     28     2.0    1.0   2.00    2.00      257     7224   0.05000V       -3.02198109    UNIFORM ‖-AXIS
 58      0.200    500      2     28     2.0    1.0   2.00    2.00       60     1708   0.65000V     -102.95525789    UNIFORM ‖-AXIS
 59      0.300    500      2     28     2.0    1.0   2.00    2.00      154     4340   0.60000V       -3.40567728    UNIFORM ‖-AXIS
 60      0.400    500      2     28     2.0    1.0   2.00    2.00       79     2240   0.65000V      -40.28712313    UNIFORM ‖-AXIS
 61      0.500    500      2     28     2.0    1.0   2.00    2.00      210     5908   0.55000V       -3.00034670    UNIFORM ‖-AXIS
 62      0.600    500      2     28     2.0    1.0   2.00    2.00       79     2240   0.65000V      -32.25789818    UNIFORM ‖-AXIS
 63      0.700    500      2     28     2.0    1.0   2.00    2.00       60     1708   0.65000V      -36.68532659    UNIFORM ‖-AXIS
 64      0.800    500      2     28     2.0    1.0   2.00    2.00       60     1708   0.65000V      -14.65270155    UNIFORM ‖-AXIS
 65      0.900    500      2     28     2.0    1.0   2.00    2.00       78     2212   0.60000V      -31.47896038    UNIFORM ‖-AXIS
 66      1.000    500      2     28     2.0    1.0   2.00    2.00      282     7924   0.35000V       -3.00151179    UNIFORM ‖-AXIS

                                           Total Function Evaluations:      180472

-----------------------------------------------------------------------------------------------------------------------------------
 54      0.900    500      2     24     2.0    1.0   2.00    2.00       60     1464   0.65000V       -3.00000000    UNIFORM ‖-AXIS
```

Table 2. CFO-PR comparative results for 23 benchmark functions (GSO/GA/PSO data from [24])

Test function	N_d	$f_{\max}$	<Best fitness>/ other algorithm	- - - - - - - - - - - - - CFO-PR - - - - - - - - - - - - -					- - - - - - CFO - - - - - -
				Best fitness	γ_{best}	Best N_p/N_d	N_{eval}		Best fitness with fixed DS boundary & fixed $N_p/N_d = 10$, $F_{rep} = 0.5$.
							Best Run	*Total*	
Unimodal functions (other algorithms: average of 1000 runs)									
f_1	30	0	$-3.6927\text{x}10^{-37}$ / PSO	$-4.8438\text{x}10^{-4}$	0.1	4	20,640	507,060	0
f_2	30	0	$-2.9168\text{x}10^{-24}$ / PSO	$-4\text{x}10^{-8}$	0.5	2	5,040	716,400	0
f_3	30	0	$-1.1979\text{x}10^{-3}$ / PSO	$-6\text{x}10^{-8}$	0.5	2	10,260	1,534,260	0
f_4	30	0	-0.1078 / GSO	$-4.2\text{x}10^{-7}$	0.5	2	5,160	332,340	0
f_5	30	0	-37.3582 / PSO	$-1.09289\text{x}10^{-3}$	0.9	6	34,560	845,640	-29
f_6	30	0	$-1.6000\text{x}10^{-2}$ / GSO	0	1.0	6	10,980	350,280	0
f_7	30	0	$-9.9024\text{x}10^{-3}$ / PSO	$-4.249\text{x}10^{-5}$	0.1	4	60,120	1,983,960	-0.002354
Multimodal functions, many local maxima (other algorithms: avg 1000 runs)									
f_8	30	12,569.5	12,569.4882 / GSO	12,569.4866	0.5	4	12,720	448,800	12,536.3016
f_9	30	0	-0.6509 / GA	$-2.05\text{x}10^{-6}$	0.7	4	16,440	680,640	0
f_{10}	30	0	$-2.6548\text{x}10^{-5}$ / GSO	$-1.5\text{x}10^{-7}$	0.5	2	5,100	904,980	0
f_{11}	30	0	$-3.0792\text{x}10^{-2}$ / GSO	$-9.97293\text{x}10^{-2}$	0.1	6	42,660	489,060	-1.4141
f_{12}	30	0	$-2.7648\text{x}10^{-11}$ / GSO	$-2.067\text{x}10^{-5}$	0.5	2	3,660	341,400	-1.7671
f_{13}	30	0	$-4.6948\text{x}10^{-5}$ / GSO	$-3.2853\text{x}10^{-3}$	0.6	6	16,920	679,620	-5.8
Multimodal functions, few local maxima (other algorithms: avg 50 runs)									
f_{14}	2	-1	-0.9980 / GSO	-0.9980	0.2	12	5,952	141,076	-1.4064
f_{15}	4	$-3.075\text{x}10^{-5}$	$-3.7713\text{x}10^{-4}$ / GSO	$-4.889\text{x}10^{-4}$	0	12	3,360	304,664	$-6.4685\text{x}10^{-3}$
f_{16}	2	1.0316285	1.031628 / GSO	1.031626	0.4	12	6,288	124,340	0.8535
f_{17}	2	-0.398	-0.3979 / GSO	-0.3979	0	8	1,872	108,340	-0.4001
f_{18}	2	-3	-3 / GSO	-3	0.9	12	1,464	180,472	-3

f_{19}	3	3.86	3.8628 / GSO	3.8627	0.2	14	3,150	200,268	3.8521
f_{20}	6	3.32	3.2697 / GSO	3.32173	0.3	12	18,072	730,212	3.3107
f_{21}	4	10	7.5439 / PSO	10.1532	0.4	6	1,896	336,712	7.7245
f_{22}	4	10	8.3553 / PSO	10.4029	0.8	6	2,208	386,176	9.4308
f_{23}	4	10	8.9439 / PSO	10.5363	0.8	6	2,256	394,320	10.1523

(N_d = Function Dimension; $f_{\max}$ = Known Global Maximum; < > Denotes Average Value)

Table 3. Number of GSO/GA/PSO Function Evaluations Per Run (from [24]).

Function	GSO/GA/PSO	Function	GSO/GA/PSO
f_1	150,000	f_{13}	150,000
f_2	150,000	f_{14}	7,500
f_3	250,000	f_{15}	250,000
f_4	150,000	f_{16}	1,250
f_5	150,000	f_{17}	5,000
f_6	150,000	f_{18}	10,000
f_7	150,000	f_{19}	4,000
f_8	150,000	f_{20}	7,500
f_9	250,000	f_{21}	10,000
f_{10}	150,000	f_{22}	10,000
f_{11}	150,000	f_{23}	10,000
f_{12}	150,000	-	-

Two columns of CFO-PR and CFO data are presented in Table 2. The CFO-PR data correspond to the best fitness returned by the single best run in the set of runs with variable N_p/N_d and variable γ . For functions f_{14} - f_{23} eleven runs were made with $0 \le \gamma \le 1$ in increments of 0.1 and $4 \le N_p/N_d \le 14$ by 2 (66 runs total). For f_1 - f_{13} the same procedure was used, but with $2 \le N_p/N_d \le 6$ by 2 (33 runs total) in order to avoid excessive runtimes. Table 2 shows the γ value corresponding to the best fitness, γ_{best} , and the corresponding best value of N_p/N_d . N_{eval} is the number of function evaluations, and it is tabulated for the single best run and for the group of runs used to determine γ_{best} and the best number of probes per axis. The CFO column contains results for runs in which pseudorandomness has been removed from the algorithm except for the probe line IPD, which was unchanged. Those runs employed fixed decision space boundaries, a fixed value of $F_{rep} = 0.5$, and a fixed value of $N_p/N_d = 10$.

Comparing CFO-PR to GSO/GA/PSO, in the first group of high dimensionality unimodal functions, f_1 - f_7, CFO-PR returned the best fitness on five of the seven functions (f_3 - f_7). PSO performed best on the first two. In the second set of high dimensionality multimodal functions with many local maxima, $f_8 - f_{13}$, CFO-PR performed best on two (f_9, f_{10}) and essentially the same as the best other algorithm (GSO) on f_8. In last group of ten multimodal functions with few local maxima, f_{14} - f_{23}, CFO-PR returned the best fitness on four (f_{20} - f_{23}), equal fitnesses on three ($f_{14,}$ $f_{17,}$ f_{18}), and very slightly lower fitnesses on the remaining three. Even though it is in its infancy, CFO-PR performed very well against three other highly sophisticated algorithms. It returned the best, equal, essentially equal, or very slightly lower fitnesses on eighteen of the twenty three test functions. It is reasonable to conclude that, overall, CFO-PR performed as well or better than GSO, which in turn performed better than PSO or GA.

Comparing CFO-PR to CFO alone (most pseudorandomness taken out), CFO alone returned the best fitness overall on f_1 - f_4, f_6, f_9, and on f_{10}. On f_{19}, GSO, CFO-PR and CFO all returned the same fitness, which happens to be the global maximum. On the other benchmarks, however, CFO with reduced pseudorandomness returned worse best fitnesses than CFO-PR. These results suggest that

CFO-PR performs better than CFO alone, but not by a wide margin.

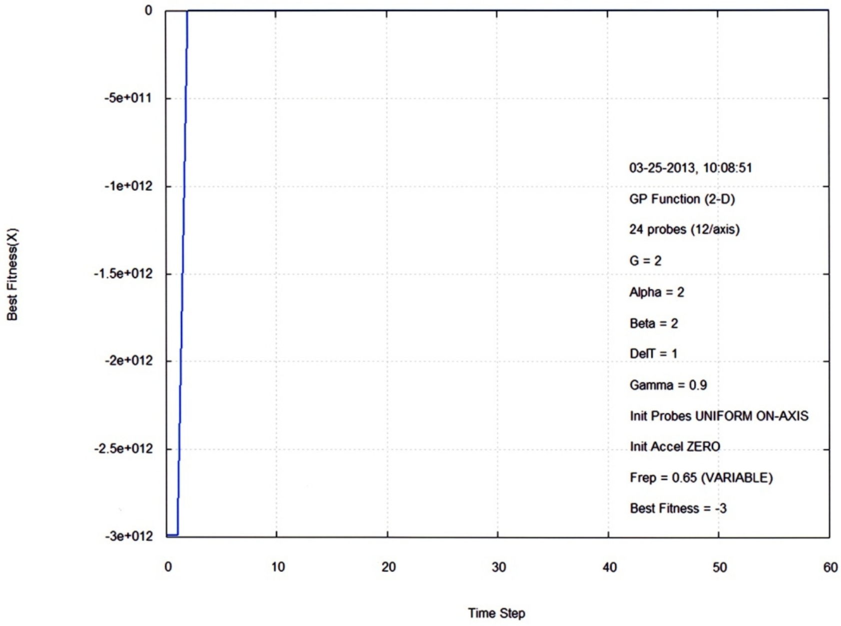

Fig. 7. Evolution of GP function best fitness

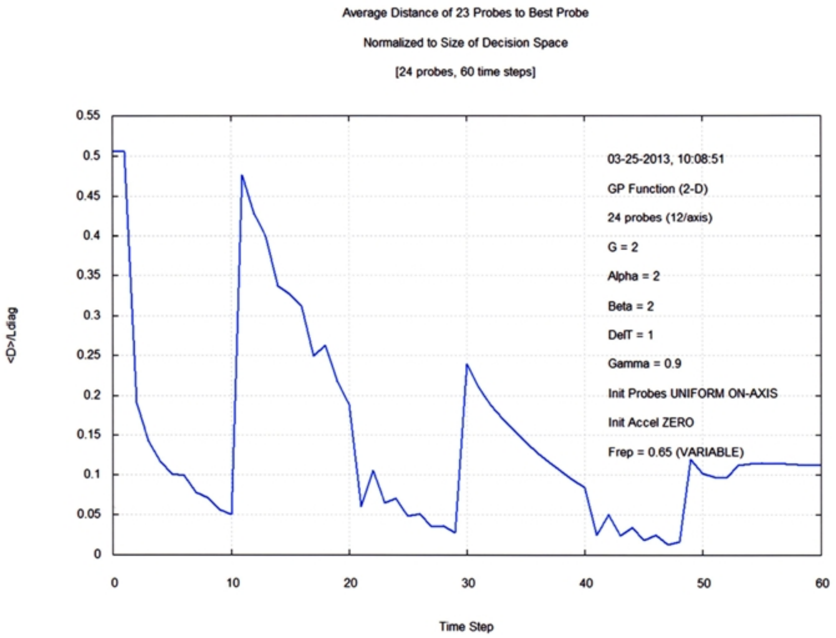

Fig. 8. Evolution of GP function D_{avg}

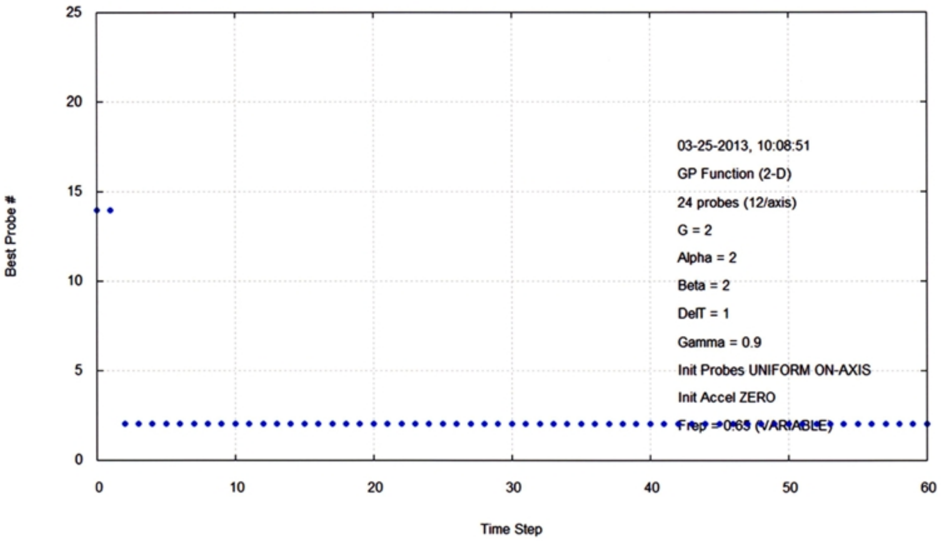

Fig. 9. GP Function best probe number

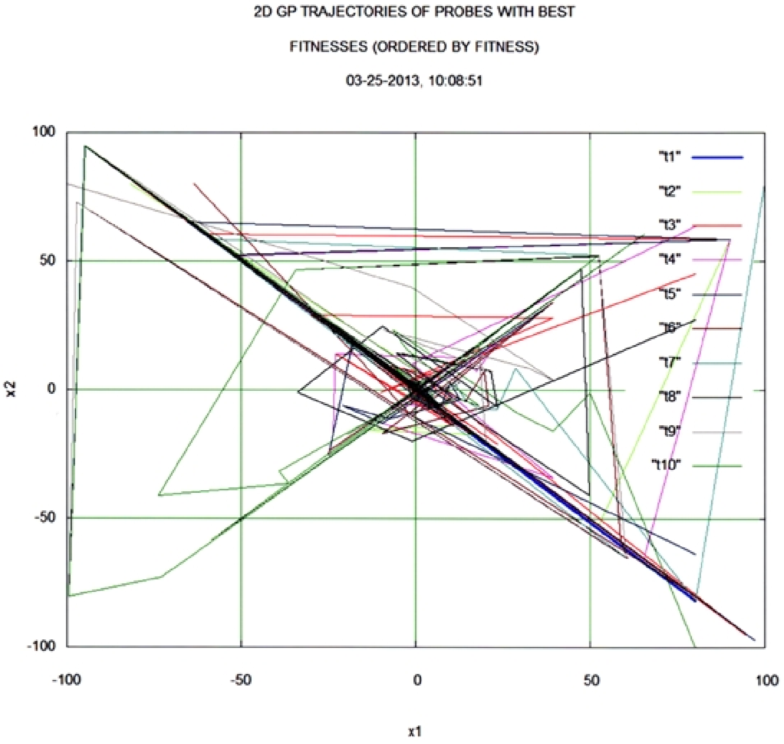

Fig. 10. GP Function trajectories of probes with best fitness

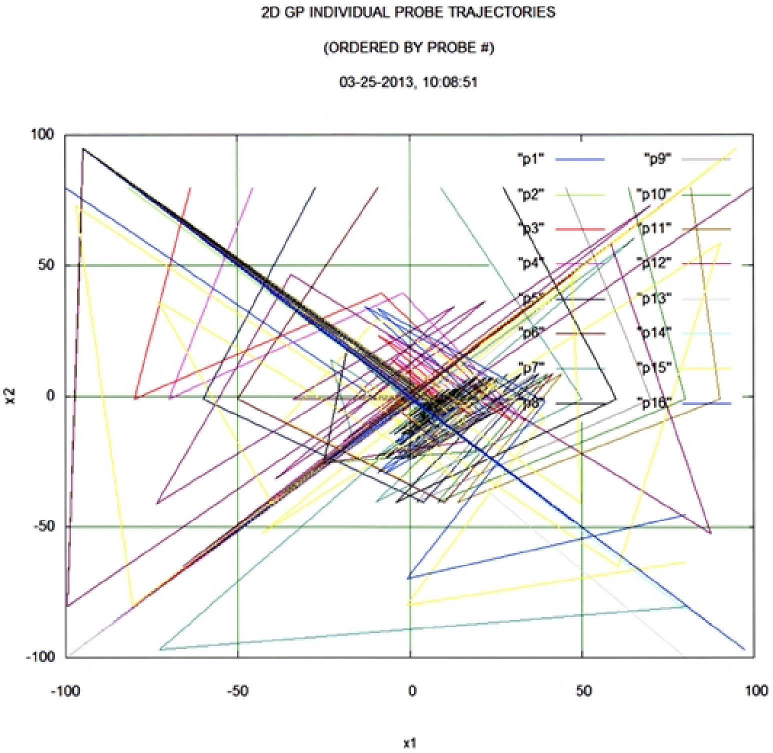

Fig. 11. GP function probe trajectories by probe number

4 Conclusion

This note suggests that pseudorandomness is an important, indeed perhaps essential, aspect of effective CFO implementations. A pseudorandom variable has an arbitrary but precisely known value that may be assigned or calculated. Its essential characteristic is that the value is uncorrelated with the decision space's topology, so that it has the effect of distributing probes pseudorandomly throughout the landscape. While in a general sense this process may appear to be similar to the randomness in an inherently stochastic algorithm, it is in fact fundamentally different. The equations underlying stochastic algorithms are formulated in terms of true random variables whose values are computed from probability distributions and consequently are unknowable until the calculation is made. Therefore successive calculations yield different values, and as a result every optimization run has a different outcome. By contrast, a pseudorandom variable in the context of CFO is known with absolute precision because of how its value is determined (assignment or deterministic calculation). This property allows CFO to compute probe trajectories precisely because it is inherently deterministic. Every CFO with the same setup, with or without a pseudorandom component, yields exactly the same results, step-by-step throughout the entire run. Importantly, CFO's reproducibility lends itself well to reactive implementations in which run parameters are tuned in response to performance metrics such as rate of convergence or fitness saturation as examples. Reactive stochastic algorithms, on the other hand, are very difficult to implement.

This paper provides examples of how pseudorandomness can improve CFO's performance. Three different approaches are used (initial probe distribution, repositioning factor, and decision space adaptation), and each was discussed in detail. A sample CFO-PR problem was presented in detail, and summary data included for a standard 23-function benchmark suite. CFO-PR's performance is quite good compared to other highly developed, state-of-the-art algorithms. In addition, data are presented for a CFO implementation in which all pseudorandomness except the IPD has been removed, and those results show that, as a general rule, injecting pseudorandomness improves CFO's performance. Hopefully these results will encourage further work on improved methodologies for injecting pseudorandomness into CFO, in particular where and how. Of course, any or all of CFO's run parameters can be pseudorandomized, not only the three considered here. But even with respect to those parameters, different approaches to how they are pseudorandomized may yield better results or faster runtimes. There are many fruitful areas of research on CFO, and it is the author's hope that this and the other CFO papers will provide the foundation and catalyst for that work.

Competing Interests

Author has declared that no competing interests exist.

References

[1] Formato RA. Central Force Optimization: A New Metaheuristic with Applications in Applied Electromagnetics. Progress In Electromagnetics Research. 2007;77:425–491.

[2] Formato RA. Parameter-Free Deterministic Global Search with Simplified Central Force Optimization. In: Huang D.-S., Zhao Z, Bevilacqua V, and Figueroa JC, editors. Advanced Intelligent Computing Theories and Applications (ICIC2010), Lecture Notes in Computer Science (LNCS 6215). Springer-Verlag Berlin Heidelberg; 2010.

[3] Formato RA. Central force optimisation: a new gradient-like metaheuristic for multidimensional search and optimisation. Int. J. Bio-Inspired Computation. 2009;1(4):217-238.

[4] Formato RA. Central Force Optimization with variable initial probes and adaptive decision space. Applied Mathematics and Computation. 2011;217(21):8866–8872.

[5] Ding D, Luo X, Chen J, Wang X, Du P, Guo Y. A Convergence Proof and Parameter Analysis of Central Force Optimization Algorithm. Journal of Convergence Information Technology (JCIT). 2011;6(10):16-23.

[6] Ding D, Qi D, Luo X, Chen J, Wang X, Du P. Convergence analysis and performance of an extended central force optimization algorithm. Applied Mathematics and Computation. 2012;219(4):2246–2259

[7] Green RC, Wang L, Alam M, Formato RA. Central Force Optimization on a GPU: A Case Study in High Performance Metaheuristics using Multiple Topologies. The Journal of Supercomputing. 2012;62(1):378-398.

[8] Green RC, Wang L, Alam M. Evaluating the Impact of Multiple Neighborhood Topologies on Central Force Optimization. Online at www.parallelcoding.com.

[9] Green R, Wang L, Alam M, Formato R. Central Force Optimization on a GPU: A case study in high performance metaheuristics using multiple topologies. IEEE Congress on Evolutionary Computation, New Orleans, June 5-8. 2011;550–557.

[10] Green R, Wang L, Alam M. Training neural networks using Central Force Optimization and Particle Swarm Optimization: Insights and comparisons, Expert Systems with Applications. 2012;39:555–563.

[11] Green R, Wang L, Alam M. Intelligent State Space Pruning with Local Search for Power System Reliability Evaluation. IEEE Power and Energy Society Innovative Smart Grid Technologies Europe, Berlin, Germany, October 2012.

[12] Haghighi A, Ramos HM. Detection of Leakage Freshwater and Friction Factor Calibration in Drinking Networks Using Central Force Optimization. Water Resource Management. 2012;26:2347–2363.

[13] Roa O, Amaya I, Ramírez F, Correa R. Solution of Nonlinear Circuits with the Central Force Optimization Algorithm. 2012 IEEE 4th Colombian Workshop on Circuits and Systems (CWCAS), Barranquilla, Colombia. 1-2 Nov 2012;1-6.

[14] Mohammad G, Dib N. Synthesis of Antenna Arrays using Central Force Optimization. Mosharaka International Conference on Communications, Computers and Applications, MIC-CPE, Amman, Jordan; 6-8 Feb 2009.

[15] Qubati GM, Formato RA, Dib NI. Antenna Benchmark Performance and Array Synthesis using Central Force Optimisation. IET Microwaves, Antennas & Propagation. 2010;4(5):583–592.

[16] Qubati GM, Dib NI. Microstrip Patch Antenna Optimization using Modified Central Force Optimization. Progress in Electromagnetics Research B. 2010;21:281-298.

[17] Montaser AM, Mahmoud KR, Elmikati HA. Tri-band Slotted Bow-Tie Antenna Design for RFID Reader using Hybrid CFO-NM Algorithm. 29th National Radio Science Conference (NRSC 2012). Giza, Egypt, April 10-12, 2012.

[18] Mahmoud KR. Central Force Optimization: Nelder-Mead Hybrid Algorithm for Rectangular Microstrip Antenna Design. Electromagnetics. 2011;31(8):578-592.

[19] Asi MJ, Dib NI. Design of Multilayer Microwave Broadband Absorbers using Central Force Optimization. Progress in Electromagnetics Research B. 2010;26:101-113.

[20] Formato RA. Improved CFO Algorithm for Antenna Optimization. Progress in Electromagnetics Research B. 2010;19:405-425.

[21] Montaser AM, Mahmoud KR, Abdel-Rahman AB, Elmikati HA. Design Bluetooth and Notched-UWB E-Shape Antenna using Optimization Techniques. Progress In Electromagnetics Research B. 2013;47:279-295.

[22] Formato RA. New Techniques for Increasing Antenna Bandwidth with Impedance Loading. Progress In Electromagnetics Research B. 2011;29:269-288.

[23] Formato RA. Improving Bandwidth of Yagi-Uda Arrays. Wireless Engineering and Technology. 2012;3(1):18-24.

[24] He S, Wu QH, Saunders JR. Group Search Optimizer: An Optimization Algorithm Inspired by Animal Searching Behavior. IEEE Trans. Evol. Computation. 2009;13(5):973-990.

[25] CIS Publication Spotlight, IEEE Comp. Intelligence Magazine. 2010;5(1):5.

[26] Yao X, Liu Y, Lin G. Evolutionary Programming Made Faster. IEEE Trans. Evol. Comp. 1999;3(2):82-102.

Appendix

CFO searches an N_d -dimensional decision space Ω for the global maxima of an objective function $f(x_1, x_2, ..., x_{N_d})$ defined on Ω : $x_i^{\min} \le x_i \le x_i^{\max}$, $1 \le i \le N_d$. The x_i are the decision variables, and i the coordinate number. The term fitness refers to the value of $f(\vec{x})$ at point $\vec{x}$ in Ω . There is no *a priori* information about the objective function's maxima, that is, $f(\vec{x})$'s topology (landscape) is unknown [1].

CFO searches Ω by flying probes through the space at discrete time steps (iterations). Each probe's location is specified by its position vector computed from two equations of motion that analogize their real-world counterparts for material objects moving through physical space under the influence of gravity without energy dissipation.

Probe p 's position vector at step j is $\vec{R}_j^p = \sum_{k=1}^{N_d} x_k^{p,j} \hat{e}_k$, where the $x_k^{p,j}$ are its coordinates and $\hat{e}_k$ the unit vector along the x_k -axis. The indices p , $1 \le p \le N_p$, and j , $0 \le j \le N_t$, respectively, are the probe number and iteration number, where N_p and N_t are the corresponding total number of probes and total number of time steps.

Equations of Motion: In metaphorical CFO space each of the N_p probes experiences an acceleration created by the gravitational pull of masses in Ω . Probe p 's acceleration at step $j-1$ is given by

$$\vec{a}_{j-1}^p = G \sum_{\substack{k=1 \\ k \ne p}}^{N_p} U(M_{j-1}^k - M_{j-1}^p) \cdot (M_{j-1}^k - M_{j-1}^p)^\alpha \times \frac{(\vec{R}_{j-1}^k - \vec{R}_{j-1}^p)}{\left\| \vec{R}_{j-1}^k - \vec{R}_{j-1}^p \right\|^\beta}, \quad (1)$$

which is the first of CFO's two equations of motion. In equation (1), $M_{j-1}^p = f(x_1^{p,j-1}, x_2^{p,j-1}, ..., x_{N_d}^{p,j-1})$ is the objective function's fitness at probe p 's location at time step $j-1$. Each of the other probes at that step (iteration) has associated with it fitness $M_{j-1}^k, k = 1,..., p-1, p+1,..., N_p$. G is CFO's gravitational constant, and $U(\cdot)$ is the Unit Step function, $U(z) = \begin{Bmatrix} 1, & z \ge 0 \\ 0, & otherwise \end{Bmatrix}$.

The acceleration $\vec{a}_{j-1}^p$ causes probe p to move from position $\vec{R}_{j-1}^p$ at step $j-1$ to $\vec{R}_j^p$ at step j according to the trajectory equation

$$\vec{R}_j^p = \vec{R}_{j-1}^p + \frac{1}{2}\vec{a}_{j-1}^p \Delta t^2, \ j \geq 1 \ , \tag{2}$$

which is CFO's second equation of motion. Note that the original CFO paper [1] included a velocity term that was set equal to zero as a matter of convenience because it simply was a additive constant in the case of rectilinear motion. Upon further consideration, however, it became clear that this term should not be included in equation (2) because, in general, a probe's motion is not rectilinear. Instead it is curvilinear, in which case the acceleration and velocity vectors are in different directions. As an example, in the case of circular motion the velocity vector is tangent to the trajectory circle while the acceleration is inwardly directed along the radius, that is, perpendicular to the velocity. This limiting case illustrates why, in general, the velocity term appearing in real-world kinematic equations should not be included in metaphorical CFO-space because it changes the direction of each probe's acceleration.

The CFO equations of motion, (1) and (2), combine to compute a new probe distribution at each time step using masses discovered by the probe distribution at the previous step. Δt is the time interval between steps during which the acceleration is constant. Note that CFO's terminology has no significance beyond reflecting CFO's kinematic roots, as does the factor ½ in eq. (2). The gravitational constant, G, and time increment, Δt, have direct analogues in Newton's equations of motion for real masses moving under real gravity through three-dimensional physical space. The CFO exponents α and β, by contrast, have no analogues in Nature. They provide added flexibility to the algorithm designer who, in metaphorical CFO space, is free to change how gravity varies with distance, or mass, or both, if doing so creates a more effective algorithm.

Mass: The concept of mass in CFO space is very important and quite different than it is in real space. Mass in the physical Universe is an inherent, immutable property of matter, whereas in CFO space it is a positive-definite user-defined function of the objective function's fitness, not necessarily the fitness itself. For example, in equation (1) mass is defined as $MASS_{CFO} = U(M_{j-1}^k - M_{j-1}^p) \cdot (M_{j-1}^k - M_{j-1}^p)^\alpha$ [difference in fitness values raised to the α power multiplied by the Unit Step]. A different function can be used if it results in a better performing CFO algorithm. In this specific implementation the Unit Step is a critical element because it prevents negative mass. Without the Unit Step CFO mass could be negative depending on which fitness is greater. But mass in the real Universe always is positive, and as a consequence the force of gravity always attractive. By contrast, mass can be positive or negative in metaphorical CFO space, depending on how it is defined, and undesirable effects may result from the wrong definition. Negative mass creates a *repulsive* gravitational force that flies probes away from maxima instead of toward them, thus defeating the very purpose of the algorithm. See [1,3] for graphical examples of the effect of repulsive gravitational force.

Errant Probes: At any iteration in a CFO run, it is possible that a probe's acceleration computed from eq. (2) may be too great to keep it inside Ω. If any coordinate $x_i < x_i^{\min}$ or $x_i > x_i^{\max}$, the probe enters a region of unfeasible solutions that are not valid for the problem at hand. The question is what to do with an errant probe, and it arises in many algorithms. There are many approaches. While many schemes are possible, a simple, empirically determined one is used here. On a coordinate-by-coordinate basis, probes flying out of the decision space are placed a fraction

$\Delta F_{rep} \le F_{rep} \le 1$ of the distance between the probe's starting coordinate and the corresponding boundary coordinate. F_{rep} is the variable repositioning factor (see, for example, [2,3] for a more detailed discussion). Its value, as well as those of all the CFO parameters, was determined empirically.

Peer-review history:
The peer review history for this paper can be accessed here (Please copy paste the total link in your browser address bar)
www.sciencedomain.org/review-history.php?iid=225&id=6&aid=1300